4-2019

The Impact of Cancer-associated Mutations in Thyroid Hormone Receptor on Its Localization

Sri Harshini Malapati

The Impact of Cancer-associated Mutations in Thyroid Hormone Receptor on Its Localization

Sri Harshini Malapati

Thesis submitted in partial fulfillment of the requirements for Undergraduate Honors in Biology from the College of William and Mary.

Accepted for Honors

Dr. Lizabeth Allison, Chair

Dr. Jordan Walk

Dr. Kurt Williamson

Dr. Patty Zwollo

College of William & Mary

Acknowledgements

Firstly, I would like to thank my mentor, Dr. Lizabeth Allison. Without Dr. Allison's guidance, completing this honors thesis would not have been possible. I have known Dr. Allison since my second semester of freshman year when I began working in her lab. Since then, Dr. Allison has encouraged me to explore my academic interests and supported me through much of what I have accomplished during my time at William & Mary. Thank you, Dr. Allison, for believing in me and always being willing to offer advice.

I would also like to thank Vinny Roggero for teaching me research techniques, helping me with fluorescence microscopy and data analysis, and clarifying my questions in lab. Thank you, Vinny, for guiding me through some of the research challenges I have faced in lab.

Lastly, I would like to thank my committee members: Dr. Jordan Walk, Dr. Kurt Williamson, and Dr. Patty Zwollo. Thank you for taking time out of your busy schedules to support me and my research. I am fortunate to have had these professors who are so committed to the success of their students.

Abstract

The thyroid hormone receptor (TR)—a nuclear receptor that is essential for the proper regulation of metabolism and development, as it regulates gene expression in response to thyroid hormone—contains nuclear localization signals (NLSs) and nuclear export signals (NESs) that allow for TR transport into and out of the nucleus, respectively. Previous research has shown that nuclear import, nuclear retention, and nuclear export of TR are associated with modulation of gene expression, the alteration of which can contribute to various diseases, including Resistance to Thyroid Hormone (RTH) Syndrome, type II diabetes mellitus, and several types of cancer. There are three main subtypes of TR: TRα1, TRβ1, and TRβ2. Here, through mammalian cell transfection of expression plasmids for green fluorescent protein (GFP)-tagged TR and fluorescence microscopy, we examined particular groups of TRα1 mutations that were observed in patients with hepatocellular carcinoma and papillary thyroid cancer and are associated with NLSs and NESs of TRα1. More specifically, we calculated the nuclear-to-cytoplasmic ratios of TRα1 variants to determine the impact of TRα1 mutations on receptor localization within HeLa cells. We found that, while wild-type TR has a primarily nuclear localization with a smooth distribution in human cells grown in culture, the TRα1 mutations S40T, K136R, L251P, V390A and A225G, D246N, G350K lead to significantly decreased nuclear-to-cytoplasmic TRα1 ratios (greater cytoplasmic distribution) and formation of TRα1 aggregates. We observed that the distribution of a TRα1 mutant with just one of the four mutations (L251P) is very similar to the distribution of the TRα1 mutant with all four mutations (S40T, K136R, L251P, V390A), suggesting that L251P plays a major role in the mislocalization of TRα1. In addition, we found that TRα1 with a G24E mutation had a significantly greater cytoplasmic distribution, compared to wild-type TRα1. In conclusion, our findings suggest that certain TRα1 mutations that are

associated with carcinoma lead to TRα1 mislocalization, which may alter the expression of thyroid hormone-dependent genes. These results contribute to an improved understanding of TR structure and function, which could lead to novel strategies for discovering therapies for TR-related illnesses.

Table of Contents

Introduction

Thyroid hormone receptor (TR) regulates processes that are essential for normal growth and development and help maintain homeostasis in adults (Zhang and Lazar, 2000). Thyroid hormone receptors are members of the nuclear receptor superfamily that serve as ligand-dependent transcription factors (Aranda and Pascual, 2001). Ligand-dependent transcription factors are proteins that modulate transcription when bound to other molecules, such as hormones, and to regulatory sequences of DNA. In the case of TR, binding of thyroid hormone (TH) to TR modulates the transcription of target genes, which allows for the synthesis of proteins that help regulate metabolism and development (Zhang and Lazar, 2000). This thesis focuses on the impact of six cancer-associated mutations in TRα1—a subtype of TR—on its localization and function.

Secretion of Thyroid Hormone

TH is secreted by the thyroid gland through hypothalamic-pituitary axis regulation. The hypothalamus secretes thyrotropin-releasing hormone (TRH), which binds to a G protein-coupled TRH receptor and stimulates the pituitary gland to release thyrotropin-stimulating hormone (TSH). TSH binds to thyroid follicular cell and induces the production and release of TH, specifically thyroxine (T_4; 3,5,3′,5′-l-tetraiodothyronine) and triiodothyronine (T_3; 3,5,3′-l-triiodothyronine). T_4 and T_3 are tyrosine-based hormones, with the numbers 3 and 4 referring to the number of iodine molecules in each compound. T_4 is thought to be a precursor molecule for T_3 which is more potent, as T_3 binds to TR and regulates transcription (Ortiga-Carvalho et al., 2011). Thyroid hormone circulates through the bloodstream by binding to a carrier protein and enters cells through membrane transporters such as the monocarboxylate transporter MCT8. After entering cells, thyroid hormones can be modified by deiodinases. Deiodinases either

activate prohormone T_4 by converting T_4 to T_3, or they inactivate T_4 by converting it to reverse T_3 (rT_3; 3,3′,5′-l-triiodothyronine) to ensure that tissues are not damaged by excess hormones (Anyetei-Anum et al., 2018). Having the proper concentration of each type of TH within cells is important because TH primarily functions by binding to thyroid hormone receptors and helps regulate gene expression.

Subtypes of Thyroid Hormone Receptors

In humans, there are two TR genes: *THRA* and *THRB*. Through differential RNA splicing, *THRA* encodes TRα1, TRα2, and TRα3 and *THRB* encodes TRβ1, TRβ2, and TRβ3. Most tissues express both TRα and TRβ, but the relative expression of these receptors depends on the type of tissue and the stage of development. For example, while TRα subtypes are more abundant in the brain, muscle, heart, bone, and gastrointestinal tract, TRβ subtypes are more abundant in the liver, kidneys, hypothalamus, pituitary, and retina (Bochukova et al., 2012).

Domains of TR

As a nuclear receptor, TR has four domains: N-terminal A/B domain, DNA-binding domain (DBD), hinge region, and C-terminal ligand-binding domain (LBD) (Figure 1). The N-terminal A/B domain is involved in the recruitment of coregulatory proteins such as coactivators and corepressors (Tsai and O'Malley, 1994). The A/B domain has the transactivation domain activation function 1 (AF1), which is responsible for transcription regulation in a ligand-independent manner (Zhang and Lazar, 2000). The A/B domain of TRα1 contains a nuclear localization signal (NLS) called NLS-2 (Mavinakere et al., 2012). The DNA-binding domain, also known as the C domain, of TR interacts with particular DNA sequences known as thyroid hormone response elements (TREs)—in the enhancer regions of target genes—via two zinc

finger motifs, ensuring that only the expression of specific genes is altered (Tsai and O'Malley, 1994). The C domain is also important for heterodimerization with retinoid X receptor (RXR), which stabilizes DNA binding (Lazar, 2003). The hinge domain, also known as the D domain, is a flexible connection between C and E/F domains that contributes to DNA binding, ligand binding, and interactions with corepressors (Nascimento et al., 2006). The hinge domain of TRα1 contains NLS-1 (Mavinakere et al., 2012). The C-terminal LBD, also known as the E/F domain, of TR binds to TH, which leads to conformational changes in TR and modifies TR activity (Tsai and O'Malley, 1994). The LBD also functions as a receptor dimerization surface that binds to coregulators, and it has an activation function 2 (AF2), which facilitates ligand-dependent transactivation (Zhang and Lazar, 2000). The LBD has three nuclear export signals (NES-H3, NES-H6, NES-H12) (Mavinakere et al., 2012).

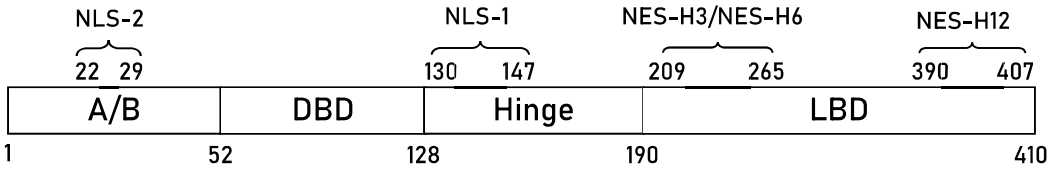

Figure 1: Domains and NLS/NES regions of TRα1.

Expression of Target Genes by TR

Once bound to DNA, TR usually heterodimerizes with RXR. When TR interacts with positive TREs and is not bound to TH, corepressors—such as histone deacetylase (HDAC), N-CoR1, or N-CoR2—are bound to TR, causing the transcription of target genes to be repressed. When TH binds to TR, TR goes through a conformational change, allowing activator proteins—such as histone acetyltransferase (HAT) and steroid receptor coactivator 1 (SRC1)—to bind to TR, which alters chromatin structure and promotes target gene expression. On the other hand, TRs

can also bind to negative TREs. In this case, corepressors are recruited to TR when bound to TH and coactivators are recruited to TR when not bound to TH (Ortiga-Carvalho et al., 2005).

Helix 12 of LBD

The LBD of TRα1 consists of 12 α-helices and undergoes ligand-dependent conformational changes. In particular, helix 12 has the ligand-dependent AF2, which mediates transactivation by RXR. Helix 12 forms two hydrophobic cavities that can bind to hormones. When TR is bound to positive TREs, helix 12 is extended and binds to a corepressor through the corepressor nuclear receptor (CoRNR) box motifs of the corepressor. Once T_3 binds, helix 12 closes around T_3 and forms a region that interacts with coactivators. Modifying the structure of helix 12 can change its specificity to and interactions with corepressors (Anyetei-Anum et al., 2018).

Nuclear Transport of TR

Thyroid hormone receptors are primarily present in the nucleus, but they are known to shuttle between the cytosol and nucleus. Specifically, approximately 90% of TRα1 is localized in the nucleus with an apparently constant shuttling of TR between the nucleus and cytoplasm. Proper nuclear export and nuclear import is crucial for the regulation of TR target gene expression.

Thyroid hormone receptor is shuttled into and out of the nucleus through nuclear pore complexes (Mavinakere et al., 2012). The nuclear pore complex (NPC)—a large assemblage of proteins that is embedded in the nuclear envelope—selectively allows for nuclear import and nuclear export of molecules that are larger than 40 kilodaltons (kDa). NPCs consist of approximately 30 types of proteins called nucleoporins (Nups), which combine to create an aqueous channel that allows certain proteins to be transported between the nucleus and cytoplasm (Beck and Hurt, 2017). These 30 proteins can be classified into three groups: the first group includes nucleoporins that

have cadherin-like domains and transmembrane α-helices, which help anchor NPCs to the nuclear envelope; the second group of nucleoporins have α-solenoid and β-propeller structures that facilitate interactions among nucleoporins; and, the third group are nucleoporins that have phenylalanine-glycine (FG)-repeats. These FG-repeats are crucial for the selective barrier function of NPCs, considering that phenylalanine and glycine are hydrophobic amino acids that interact with each other and with transport proteins that carry molecules into and out of NPCs (Devos et al., 2006).

While nucleocytoplasmic transport of ions and molecules that are less than 40 kDa occurs through passive diffusion, transport of molecules that are larger than 40 kDa requires receptor-mediated translocation (Veldman and Yang, 2017). Nuclear transport proteins, which include importins and exportins, are known as karyopherins. Karyopherins recognize nuclear localization signals (NLSs) (for import of molecules into the nucleus) and nuclear export signals (NESs) (for export of molecules out of the nucleus) (Cook et al., 2007).

Nuclear Import: An importin binds to the NLS of a cargo protein in the cytoplasm and passes through a nuclear pore complex. Once the bound importin enters the nucleus, it interacts with RanGTP and undergoes a conformational change which causes the importin to detach from the cargo protein. The importin-RanGTP complex then goes to the cytoplasm, where RanGAP—a GTPase-activating protein that is located in the cytoplasm—and Ran-binding proteins interact with the complex to hydrolyze GTP. GTP hydrolysis converts RanGTP to RanGDP. The RanGDP-importin complex disassembles, allowing the importin to be available for the nuclear import of another protein. RanGDP then binds to a nuclear transport factor and returns to the nucleus, where a guanine nucleotide exchange factor (GEF) replaces the GDP in RanGDP with GTP, creating RanGTP (Cook et al., 2007).

Nuclear export: In the nucleus, an exportin binds to the NES of a cargo protein. RanGTP binds to the exportin-cargo complex in the nucleus, forming a trimeric complex that stabilizes nuclear export. The trimeric complex exits the nucleus via the nuclear pore complex. In the cytoplasm, RanGTP binds to RanGAP which hydrolyzes GTP, allowing the trimeric complex to dissociate. The RanGDP returns to the nucleus where it interacts with GEF to form RanGTP (Cook et al., 2007).

Protein aggregation

Protein aggregation occurs when misfolded proteins interact with one another and accumulate either within or outside the cell. After being synthesized, proteins normally fold into thermodynamically favorable three-dimensional structures in the cytoplasm. In this case, the hydrophobic parts of the proteins interact with one another and shield themselves from the hydrophilic aqueous surroundings by clustering towards the center of the protein. These interactions mean that the outside portion of the folded protein is mostly hydrophilic while the inside of the protein is mostly hydrophobic (Dobson, 2003).

In addition to the covalent peptide bonds between amino acids, the structures of proteins depend on non-covalent interactions and di-sulfide bonds within and between proteins. When non-covalent interactions change, which can occur due to mutations, the protein can be misfolded. If the protein does not refold into its native state, proteins can aggregate (Dobson, 2003). Such protein aggregation has been previously shown to contribute to the progression of diseases, including neurodegenerative diseases and cancer (Jucker and Walker, 2013).

Nongenomic Effects of TR

In addition to the genomic impacts of thyroid hormone, increasing evidence is emerging of nongenomic impacts via receptors in the plasma membrane, mitochondria, and cytoplasm, which can be structurally homologous to nuclear receptors (Davis et al., 2016). These nongenomic impacts include organization of microfilaments, cell proliferation, and angiogenesis, further supporting the hypothesis that TR mutations can impact cancer development (Kalyanaraman et al., 2014).

Relevance of TR Mutations

Mutated TR was first thought to be associated with cancer after it was discovered that v-ErbA—a retroviral oncoprotein that contributes to carcinogenesis in chickens infected with avian erythroblastoma virus (AEV)—is a dominant negative mutant of chicken wild-type TRα1. Many TR mutants that are associated with disease states are unable to bind to T_3, which disrupts proper target gene transcription. In addition, mutant TR may display dominant negative activity, in which case the mutant TR competes with wild-type TR for DNA binding and prevents normal transcriptional activity (Bonamy et al., 2005). TR mutants with dominant negative activity were found to be mislocalized to the cytoplasm and form aggresomes (Bondzi et al., 2011). Considering that these target genes are linked to development, metabolism, and growth, such alterations in the cellular distribution of TR may be contributing to the development of particular types of cancer, including hepatocellular carcinoma and papillary thyroid cancer.

This thesis focuses on describing six cancer-associated TRα1 mutants: S40T, K136R, L251P, V390A; L251P; A225G, D246N, E350K; E213D; G24E; and K74E (Figure 2, Table 1).

	TRα1 Mutation	TRα1 Domain	Original Amino Acid	New Amino Acid
Mutant 1	S40T	A/B Domain	Serine	Threonine
	K136R	Hinge Domain	Lysine	Arginine
	L251P	LBD	Leucine	Proline
	V390A	LBD	Valine	Alanine
Mutant 2	**L251P**	LBD	Leucine	Proline
Mutant 3	**A225G**	LBD	Alanine	Glycine
	D246N	LBD	Aspartic Acid	Asparagine
	E350K	LBD	Glutamic Acid	Lysine
Mutant 4	**E213D**	LBD	Glutamic Acid	Aspartic Acid
Mutant 5	**G24E**	A/B Domain	Glycine	Glutamic Acid
Mutant 6	K74E	DBD	Lysine	Glutamic Acid

Table 1: Amino acid names of TRα1 mutations. The mutations in bold are located in the NLSs/NESs of TRα1.

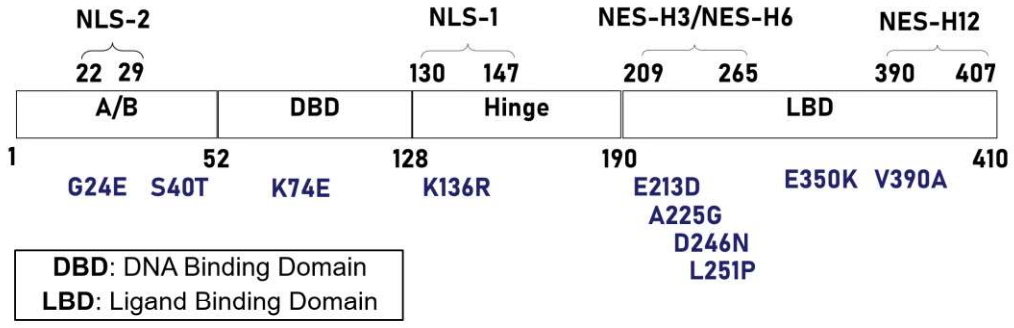

Figure 2: Location of cancer-associated mutations relative to TRα1 domains.

Contexts of TR Mutations

The TRα1 mutations described in this thesis were identified in patients with either hepatocellular carcinoma (HCC) or papillary thyroid cancer. While high levels of mutations were observed in tumor lesions, no mutations were identified in the patients' normal tissues, suggesting a correlation between TRα1 mutations and the development of particular types of cancer (Lin et al., 1999).

TRα1 (S40T, K136R, L251P, V390A): K136R, L251P, V390A are point mutations in NLS-1, NES-H3/H6, and NES-H12 regions of TRα1. S40T is a mutation in the A/B domain of TRα1 but does not correspond to a known NLS or NES. The four point mutations were identified in a patient's HCC tissues by using mismatch RNA analysis. This patient did not express truncated forms of TRα1, as determined by RT-PCR after isolating truncated TR mRNAs from the patient's hepatoma cells. TRα1 expression in the HCC tissues of this patient was normal. This TRα1 mutant's T_3-binding activity was completely lost, while its DNA-binding activity was normal (Lin et al., 1999).

TRα1 (A225G, D246N, G350K): A225G and D246N are point mutations in the NES-H3/H6 region of TR. G350K is located in the LBD of TR, but it is not in an NLS or NES region. The three point mutations were identified in a patient's HCC tissues by using mismatch RNA analysis. When total RNAs were isolated from this patient's tumors, truncated TRα1 was found to be expressed along with full-length TRα1. The TRα1 mutant showed a lack of T_3-binding activity but normal DNA binding (Lin et al., 1999).

TRα1 (G24E): G24E is a point mutation in the NLS-2 region of TR. The mutations were identified in a patient's HCC tissues by using mismatch RNA analysis. G24E is one of the four

mutations (G24E, M256V, E343A, P269L) identified in the patient's tumor. This patient's tumor showed expression of both truncated forms of TRα1 and full-length TRα1. The TRα1 mutant had a lack of T_3-binding activity but normal DNA-binding activity (Lin et al., 1999).

TRα1 (E213D): E213D is a point mutation in the NES-H3/H6 region of TR. This mutation was found in a tissue obtained from thyroidectomy which was performed following cancer diagnosis; histological evaluation confirmed that the patient had papillary thyroid cancer. RNAs were isolated from the tumor and mutations were identified through DNA sequencing. Along with the E213D amino acid substitution in TRα1, this patient's tissue had two TRβ1 mutations (E34G and P141L). The TRα1 mutant and TRβ1 mutant showed impaired transcriptional activity and dominant negative activity (Puzianowska-Kuznicka et al., 2002).

TRα1 (K74E): K74E is a point mutation in the DBD of TRα1 that was identified in a patient whose HCC tissues consisted of two mutations (K74E and A264V). The mutations were identified by using mismatch RNA analysis. This patient's tumor did not express truncated forms of TRα1 or TRβ1. The TRα1 mutant showed a lack of T_3-binding and DNA-binding activities (Lin et al., 1999).

Methods

Synthetic gene constructs

Wild-type TRα1 and mutant TRα1 constructs with antibiotic-resistance were made by GeneArt Gene Synthesis. These gene sequences were cloned into a green fluorescent protein (GFP) plasmid vector or red fluorescent protein (mCherry) plasmid vector. The expression plasmid for caveolin-1, CAV1-mCherry, was a gift from Ari Helenius (Addgene plasmid #27705). Expression of fluorescent fusion proteins allowed TRα1 and caveolin-1 to be visualized via fluorescence microscopy.

Preparation of Plasmid DNA

For transformation of plasmids into host bacteria, 1 ng of plasmid DNA was added to competent *E. coli* cells that were thawed on ice for 10 minutes. The tube containing the DNA-*E. coli* mixture was flicked 5 times to ensure that cells adequately mixed with the plasmid DNA. This tube was placed on ice for 30 minutes, transferred to a 42 °C water bath for 30 seconds, and placed back on ice for 5 minutes; this process, which is known as the heat shock method, allows the plasmid DNA to be taken up by cells. This mixture was then transferred to a 15 mL tube and 950 µL of room temperature SOC was pipetted into the tube. The 15 mL tube was placed in a 37 °C shaking incubator (250 revolutions per minute) for 60 minutes. Meanwhile, antibiotic-agar plates were warmed in a 37 °C incubator for approximately 45 minutes. 100 µL of cell mixture was spread onto a warmed antibiotic-agar plate and incubated at 37 °C overnight; this process allows the cells and, thus, the plasmids that were taken up by the cells to multiply.

Single colonies of *E. coli* cells from antibiotic-agar plates were added to a mixture containing 3 mL of LB media and 30 µg/mL of the specific antibiotic used in the antibiotic-agar plates; using

single colonies increases the likelihood of all plasmids having the same DNA sequence. These cultures were placed in a 37 °C shaking incubator (300 revolutions per minute) for 8 hours. 1 mL of this culture was added to 50 mL of LB media and 30 μg/mL of the specific antibiotic. This mixture was placed in a 37 °C shaking incubator (300 revolutions per minute) overnight. Then, cultures were centrifuged for 10 minutes at 6000 x g at 4 °C. Zymo Research Zyppy™ Plasmid Midiprep Kits were used to extract plasmids from the cell pellets. The purity of these plasmids was determined by utilizing a Nanodrop® 1000 spectrophotometer.

Preparation of HeLa cells

HeLa cells were cultured in Nunc filter-capped flasks containing Gibco Minimum Essential Medium (MEM) with Invitrogen 10% fetal bovine serum (FBS). Cells were grown in a ThermoScientific incubator at 37 °C under 98% humidity and 5% CO_2.

Seeding and Transfection of HeLa Cells

In preparation for transfection, approximately $2.5x10^5$ HeLa cells were added onto Fisher glass coverslips in each of the wells in a 6-well plate and incubated overnight at 37 °C. The next day, 2 μg-4 μg of plasmid DNA (the quantity of which varied based on the experiment) were added to Opti-MEM such that the combined volume of plasmid DNA and Opti-MEM equaled 250 μL. In addition, 8 μL of Lipofectamine 2000 were added to 242 μL of Opti-MEM. Both mixtures were incubated at room temperature separately for 5 minutes. Then, both mixtures were combined and incubated at room temperature for 20 minutes. 500 μL of the combined mixture was added to each of the wells in the 6-well plate. After incubating the 6-well plate at 37 °C for 6-8 hours, the media was aspirated, and 2 mL of MEM with FBS was pipetted into each well. The 6-well plate was again placed in the 37 °C incubator overnight.

Fixation of HeLa Cells

Twenty-four hours after transfection, MEM with FBS was aspirated off the wells, and the HeLa cells were washed with 2 mL of D-PBS for 10 seconds three times. In a Fisher Hamilton fume hood, 2 mL of 3.7% formaldehyde solution diluted in 1x D-PBS was added to each well. After 9 minutes, the formaldehyde solution was pipetted out of each well. The cells were again washed three times with 2 mL of 1x D-PBS for 5 minutes. Using tweezers, coverslips were mounted onto glass slides using Fluoro-Gel II with DAPI. The slides were kept in a microscope slide box at 4 °C for at least 24 hours prior to scoring.

Fluorescence Microscopy

Glass slides were blinded and examined under an inverted fluorescence microscope using Nikon NIS-Elements microscope imaging software on a computer. In the NIS-Elements program, two small rectangular Regions of Interest (ROI) were inserted onto a fluorescent cell, with one ROI in the nucleus and one in the cytoplasm. To more accurately quantify the intensity of fluorescence in the nucleus and cytoplasm, ROIs were placed on representative portions of cells. For each experiment, 3-4 biologically independent replicates were performed with a minimum of 100 cells analyzed per slide. The ratio of nuclear fluorescence intensity to cytoplasmic fluorescence intensity was determining by analyzing the data in Microsoft Excel. The difference between nuclear and cytoplasmic fluorescence intensity was analyzed for statistical significance by using Student's T-test, with p-value of less than 0.05 considered significant.

Confocal Microscopy and Colocalization

Glass slides were blinded and examined under a confocal microscope using Nikon NIS-Elements microscope imaging software on a computer. Confocal microscopy is a form of fluorescence

microscopy that allows for three-dimensional examination of cells and the generation of high-resolution images. Galvano setting was used to obtain higher quality images of cells. One small rectangular ROI was inserted onto an area of a cell that had both green fluorescence and red fluorescence to determine colocalization. Three biologically independent replicates were conducted for each experiment with a minimum of 25 cells analyzed per slide. Pearson's Correlation Coefficient was used to determine whether there was significant colocalization between two proteins.

Results

TRα1 S40T, K136R, L251P, V390A; TRα1 A225G, D246N, E350K; and TRα1 G24E have significantly lower nuclear-to-cytoplasmic ratios than wild-type TRα1

Since the mutations K136R, L251P, V390A, A225G, D246N, and G24E are all located within known NLS/NES regions of TRα1, it was predicted that the cellular distribution of these TRα1 mutants would be different from that of wild-type (WT) TRα1. HeLa cells were transfected with GFP-WT TRα1, GFP-TRα1 G24E, GFP-TRα1 A225G, D246N, E350K, and GFP-TRα1 S40T, K136R, L251P, V390A expression plasmids, fixed, and stained with DAPI, and analyzed by quantitative fluorescence microscopy to calculate the relative nuclear-to-cytoplasmic ratio (Figure 3). Using Student's T-test, it was found that TRα1 G24E showed a significantly lower relative nuclear-to-cytoplasmic ratio (greater cytosolic population) than WT TRα1 ($p=0.0349$). The relative nuclear-to-cytoplasmic ratio of TRα1 A225G, D246N, E350K was significantly lower than that of wild-type TRα1 within HeLa cells ($p<0.0001$). TRα1 S40T, K136R, L251P, V390A cells also showed a significantly lower nuclear-to-cytoplasmic ratio than wild-type cells ($p<0.0001$).

(A)

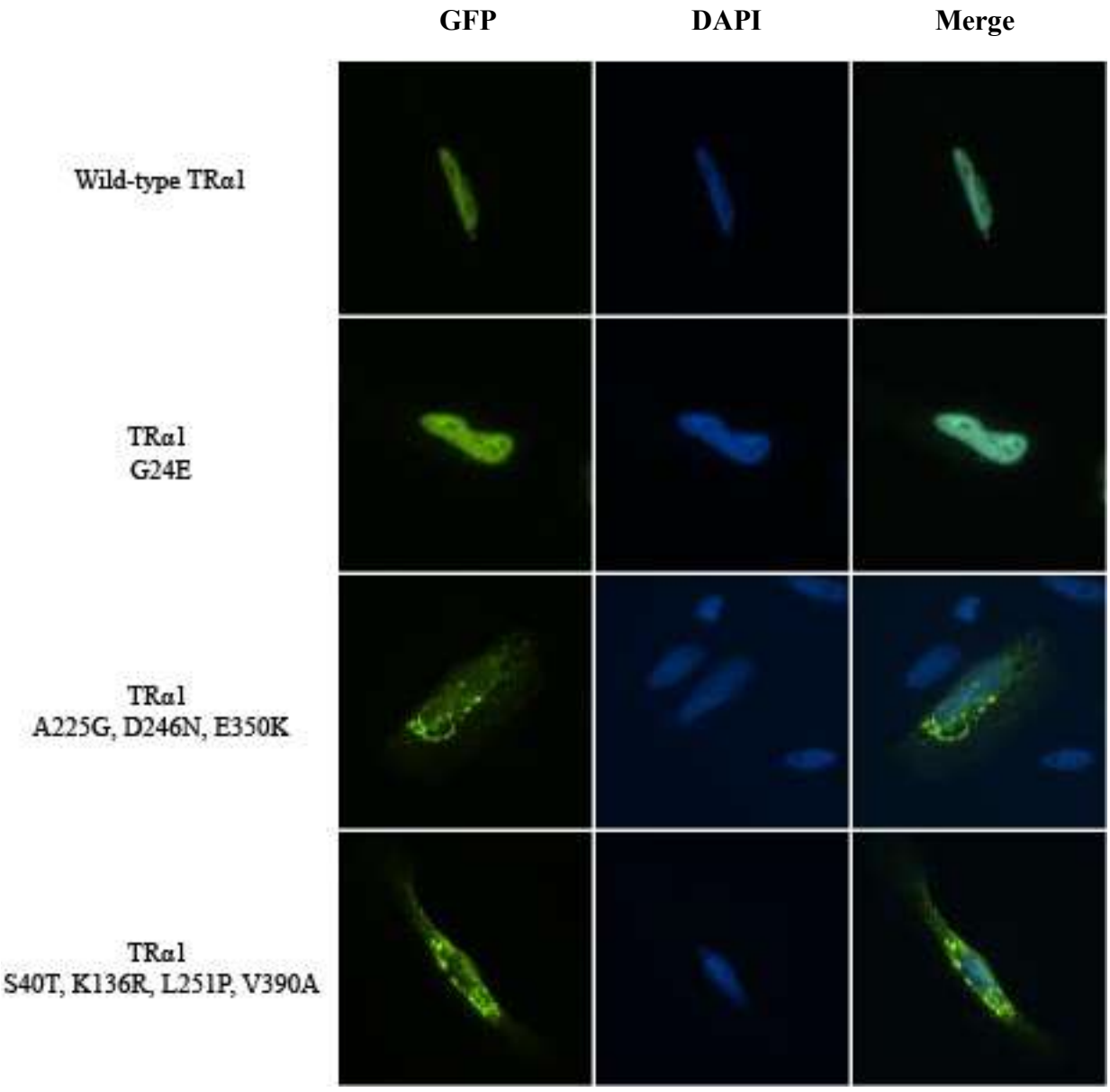
GFP
DAPI
Merge
Wild-type TRα1
TRα1
G24E
TRα1
A225G, D246N, E350K
TRα1
S40T, K136R, L251P, V390A

(B)

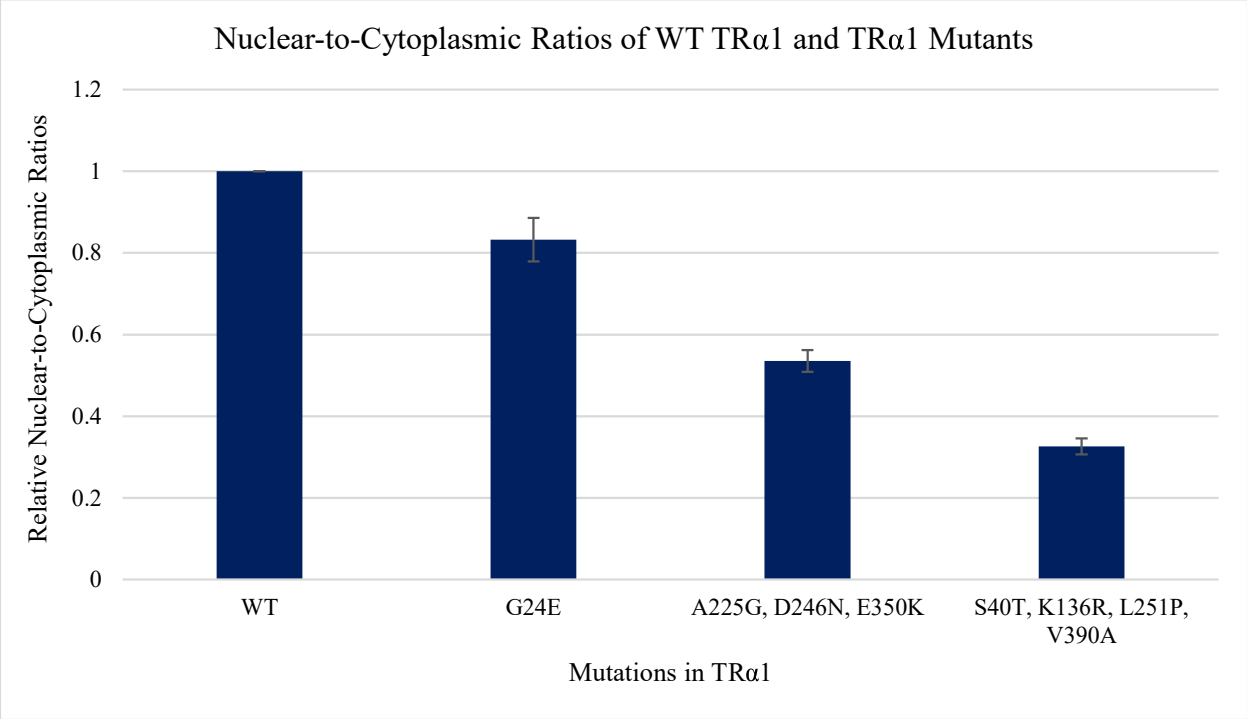

Figure 3: HeLa cells were transfected with GFP-WT TRα1, GFP-TRα1 G24E, GFP-TRα1 A225G, D246N, E350K, and GFP-TRα1 S40T, K136R, L251P, V390A expression plasmids, fixed, and stained with DAPI, and analyzed by quantitative fluorescence microscopy. (A) In the images, green fluorescence indicates GFP-TRα1 and blue fluorescence indicates the DAPI-stained nucleus. (B) In the graph, the bars indicate the relative N/C for mutant TRα1, normalized to the N/C ratio of wild-type, where wild-type was set at 1.0. Error bars indicate ± SEM (n=3-4 biologically independent replicates, 100 cells scored per replicate).

Nuclear-to-cytoplasmic ratios of TRα1 E213D and TRα1 K74E are not significantly different from that of wild-type TRα1

Since the mutation E213D is located in an NES region of TRα1, it was predicted that the cellular distribution of this TR mutant would be significantly different from that of WT TRα1. Since K74E is not in an NLS/NES region, it was predicted that its nuclear-to-cytoplasmic ratio would not be significantly different from that of WT TRα1. Nonetheless, TRα1 K74E was examined because previous research found that K74 is conserved in the DBD of TRα1 and functions as an allosteric sensor that is involved in transcription regulation after binding to DNA. HeLa cells were transfected with GFP-WT TRα1, GFP-TRα1 E213D, and GFP-TRα1 K74E expression plasmids, fixed, and stained with DAPI, and analyzed by quantitative fluorescence microscopy to calculate the relative nuclear-to-cytoplasmic ratio (Figure 4). Using Student's T-test, it was found that the relative nuclear-to-cytoplasmic ratios of WT TRα1 and TRα1 E213D were not significantly different ($p=0.8554$). The relative nuclear-to-cytoplasmic ratios of WT TRα1 and TRα1 K74E also were not significantly different ($p=0.5464$).

(A)

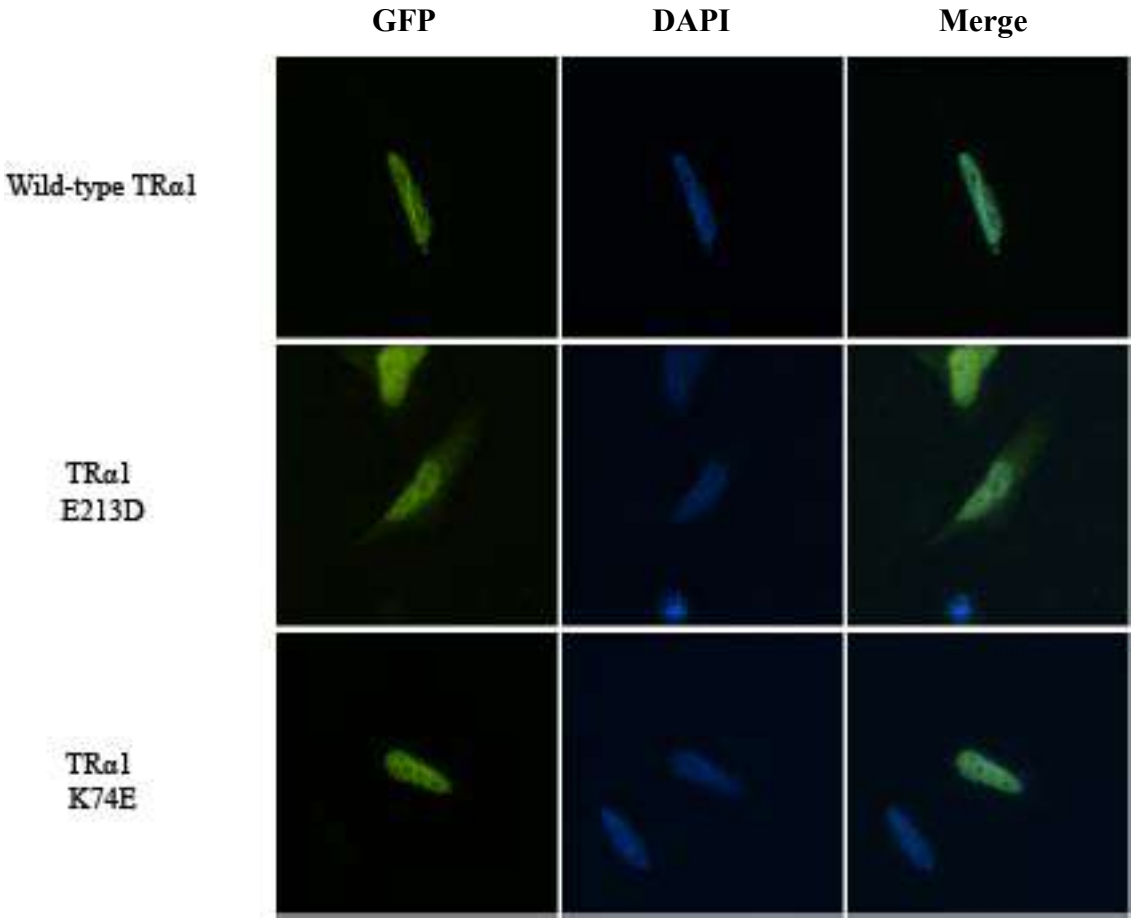

(B)

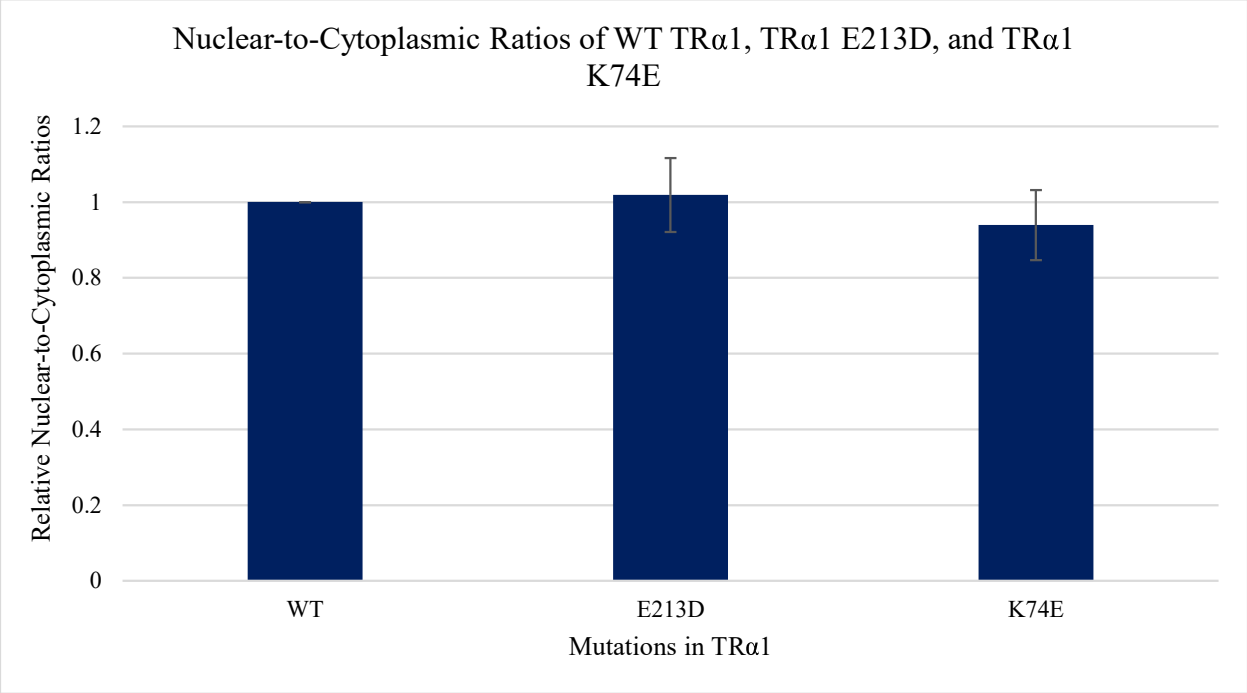

Figure 4: HeLa cells were transfected with GFP-WT TRα1, GFP-TRα1 E213D, and GFP-TRα1 K74E expression plasmids, fixed, and stained with DAPI, and analyzed by quantitative fluorescence microscopy. (A) In the images, green fluorescence indicates GFP-TRα1 and blue fluorescence indicates DAPI-stained nucleus. (B) In the graph, the bars indicate the relative N/C for mutant TRα1, normalized to the N/C ratio of wild-type, where wild-type was set at 1.0. Error bars indicate ± SEM (n=3 biologically independent replicates, 100 cells scored per replicate).

Nuclear-to-cytoplasmic ratio of TRα1 L251P is not significantly different from that of TRα1 S40T, K136R, L251P, V390A

In order to determine which of the four mutations in TRα1 S40T, K136R, L251P, V390A was leading to TR mislocalization, TRα1 expression plasmid with just one of the four mutations (TRα1 L251P) was transfected into HeLa cells. L251P was chosen to be examined initially because the change from lysine (positively charged) to proline (neutral and forms kinks in α-helices) is more likely to alter TRα1 structure and function than the change from lysine (positively charged) to arginine (positively charged) or the change from valine (nonpolar) to alanine (nonpolar). HeLa cells were transfected with GFP-WT TRα1, GFP-TRα1 S40T, K136R, L251P, V390A, and GFP-TRα1 L251P expression plasmids, fixed, and stained with DAPI, and analyzed by quantitative fluorescence microscopy to calculate the relative nuclear-to-cytoplasmic ratio (Figure 5). Using Student's T-test, it was found that TRα1 L251P cells showed a significantly lower relative nuclear-to-cytoplasmic ratio (greater cytoplasmic population) than WT TRα1 cells ($p<0.0001$). Relative nuclear-to-cytoplasmic ratios in TRα1 S40T, K136R, L251P, V390A cells and in TRα1 L251P cells were not significantly different ($p=0.3750$).

(A)

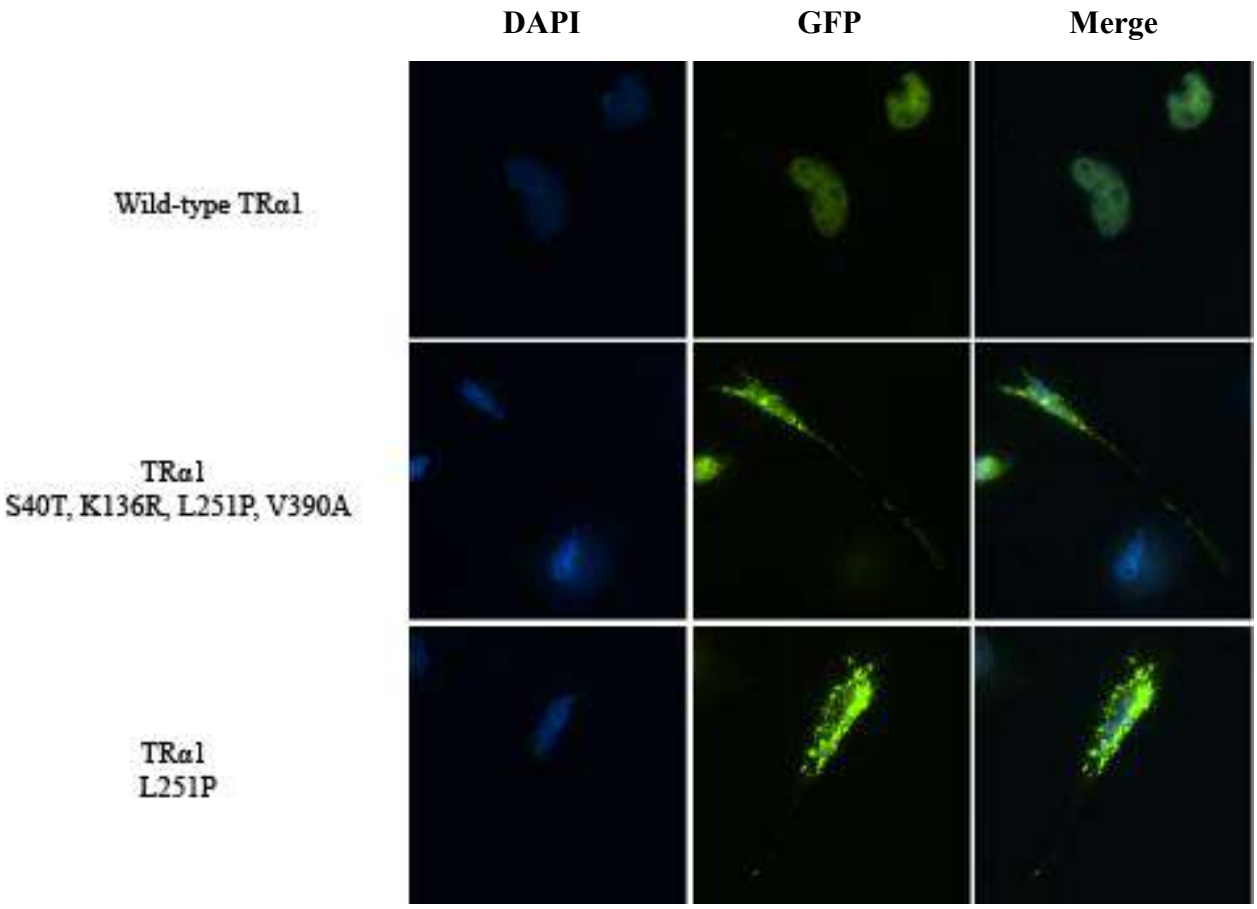
DAPI
GFP
Merge
Wild-type TRα1
TRα1
S40T, K136R, L251P, V390A
TRα1
L251P

(B)

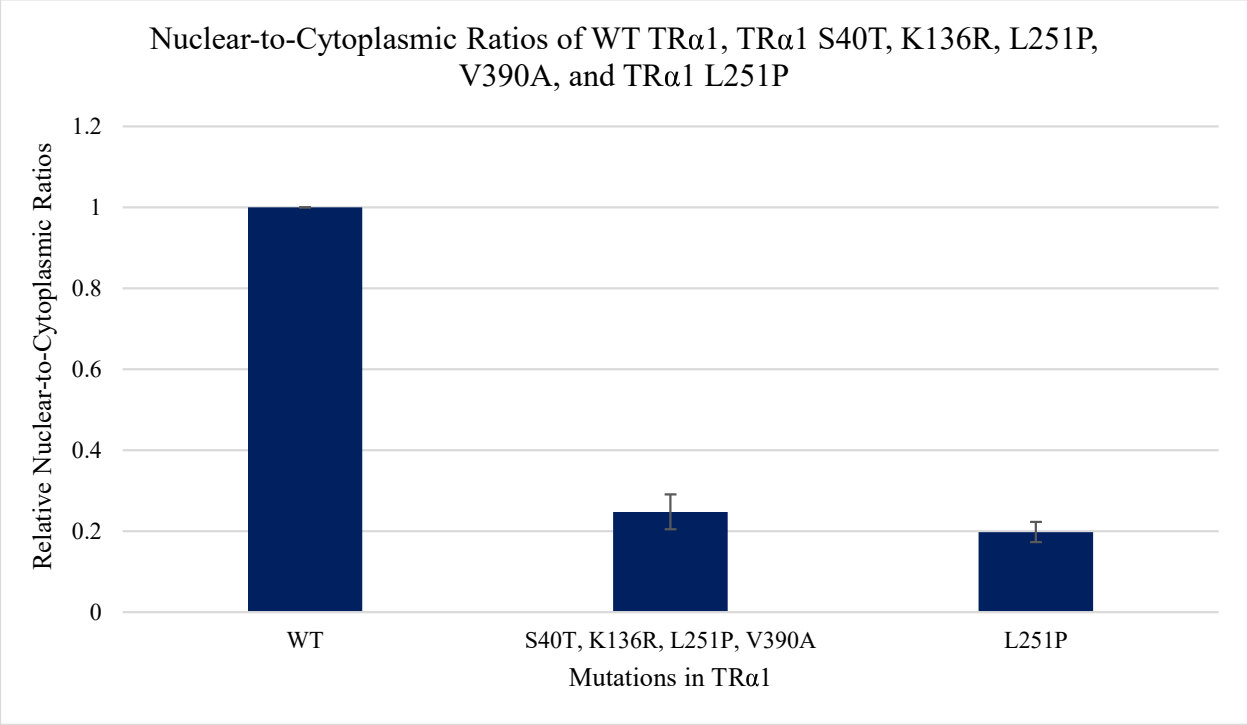

Figure 5: HeLa cells were transfected with GFP-WT TRα1, GFP-TRα1 S40T, K136R, L251P, V390A, and GFP-TRα1 L251P expression plasmids, fixed, and stained with DAPI, and analyzed by quantitative fluorescence microscopy. (A) In the images, green fluorescence indicates GFP-TRα1 and blue fluorescence indicates DAPI-stained nucleus. (B) In the graph, the bars indicate the relative N/C for mutant TRα1, normalized to the N/C ratio of wild-type, where wild-type was set at 1.0. Error bars indicate ± SEM (n=3 biologically independent replicates, 100 cells scored per replicate).

A significantly higher percentage of cells with TRα1 S40T, K136R, L251P, V390A and TRα1 A225G, D246N, E350K have aggregates than cells with wild-type TRα1

When TRα1 S40T, K136R, L251P, V390A and TRα1 A225G, D246N, E350K were examined for alteration of cellular distribution, it was found that the TRα1 mutants were forming more aggregates throughout the cells. HeLa cells were transfected with GFP-WT TRα1, GFP-TRα1 S40T, K136R, L251P, V390A, and GFP-TRα1 A225G, D246N, E350K expression plasmids, fixed, and stained with DAPI, and analyzed by quantitative fluorescence microscopy to calculate the percentage of cells with or without aggregates (Figure 6). Using Student's T-test, it was found that the percentage of cells with smooth distribution is significantly higher among cells with WT TRα1 than among cells with TRα1 mutants ($p<0.0005$).

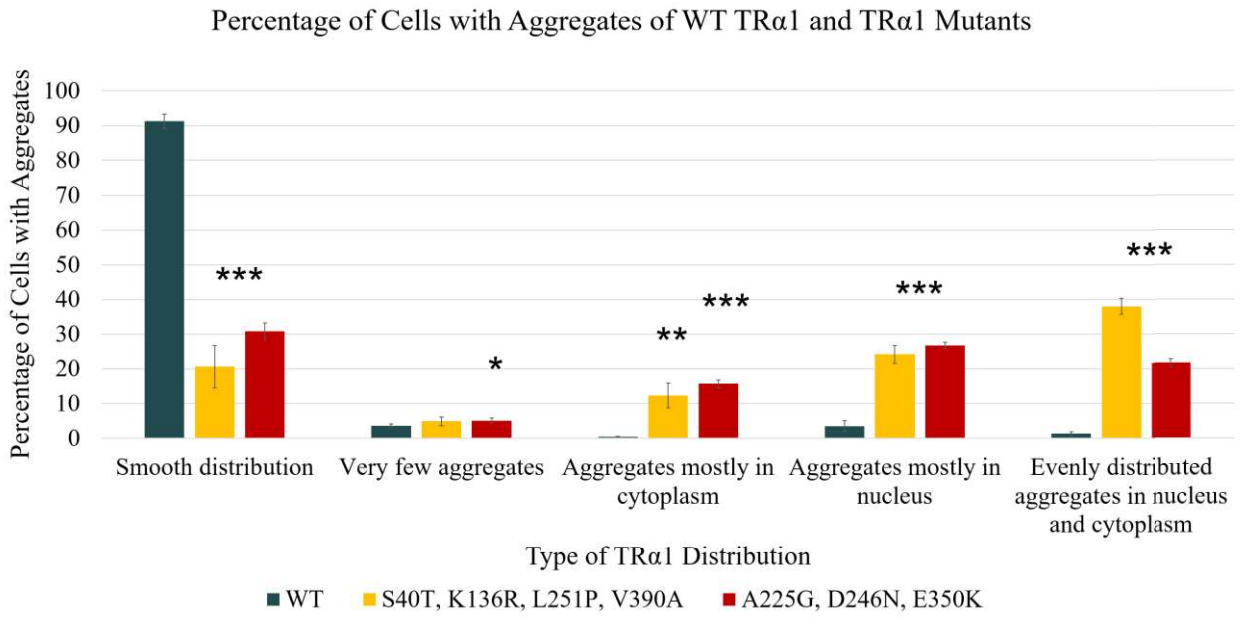

Figure 6: HeLa cells were transfected with GFP-WT TRα1, GFP-TRα1 S40T, K136R, L251P, V390A, and GFP-TRα1 A225G, D246N, E350K expression plasmids, fixed, and stained with DAPI, and analyzed by quantitative fluorescence microscopy. Error bars indicate ± SEM (*=$p \leq 0.05$, **=$p \leq 0.005$, ***=$p \leq 0.0005$; Student's T-test) (n=3-4 biologically independent replicates, 100 cells analyzed per replicate).

TRα1 S40T, K136R, L251P, V390A is not significantly colocalized with Caveolin-1

Caveolin-1, a protein encoded by the *CAV1* gene, is involved in numerous biological processes including transcytosis, endocytosis, and tumor suppression. In one study, analysis of tissue samples from 160 HCC patients showed that patients with strong caveolin-1 expression had decreased overall survival rate. Overexpression of caveolin-1 has been repeatedly implicated in the angiogenesis and metastasis of hepatocellular carcinoma, as it increases cell growth and invasiveness of tumors (Tang et al., 2012). In another study, it was shown that a particular truncated TRα1 isoform colocalizes with caveolin-1 in the plasma membrane (Hayer et al., 2010). Along with the evidence linking caveolin-1, TRα1, and hepatocellular carcinoma, the cellular distribution of TRα1 S40T, K136R, L251P, V390A appeared to be similar to that of caveolin-1. Thus, the possibility of colocalization of the TR mutant and caveolin-1 was tested through confocal microscopy. Pearson's correlation coefficient (PCC), which is denoted by *r*, was used to quantify colocalization. PCC can range from +1 to -1, with a value of 0 suggesting a lack of colocalization and a value of 1 indicating perfect colocalization. It is accepted that an r value of ≥0.5 indicates significant colocalization (Adler and Parmryd, 2010).

HeLa cells were transfected with mCherry-caveolin-1 and GFP-TRα1 S40T, K136R, L251P, V390A expression plasmids, fixed, and stained with DAPI, and analyzed by confocal microscopy to determine if caveolin-1 and TRα1 S40T, K136R, L251P, V390A are colocalized (Figure 7). Upon calculating PCC, it was found that caveolin-1 and TRα1 S40T, K136R, L251P, V390A are not colocalized (r=0.2705). Pearson's correlation coefficient of cells with only Caveolin-1 or cells with only TRα1 S40T, K136R, L251P, V390A were 0.0776 and 0.1266, respectively.

(A)

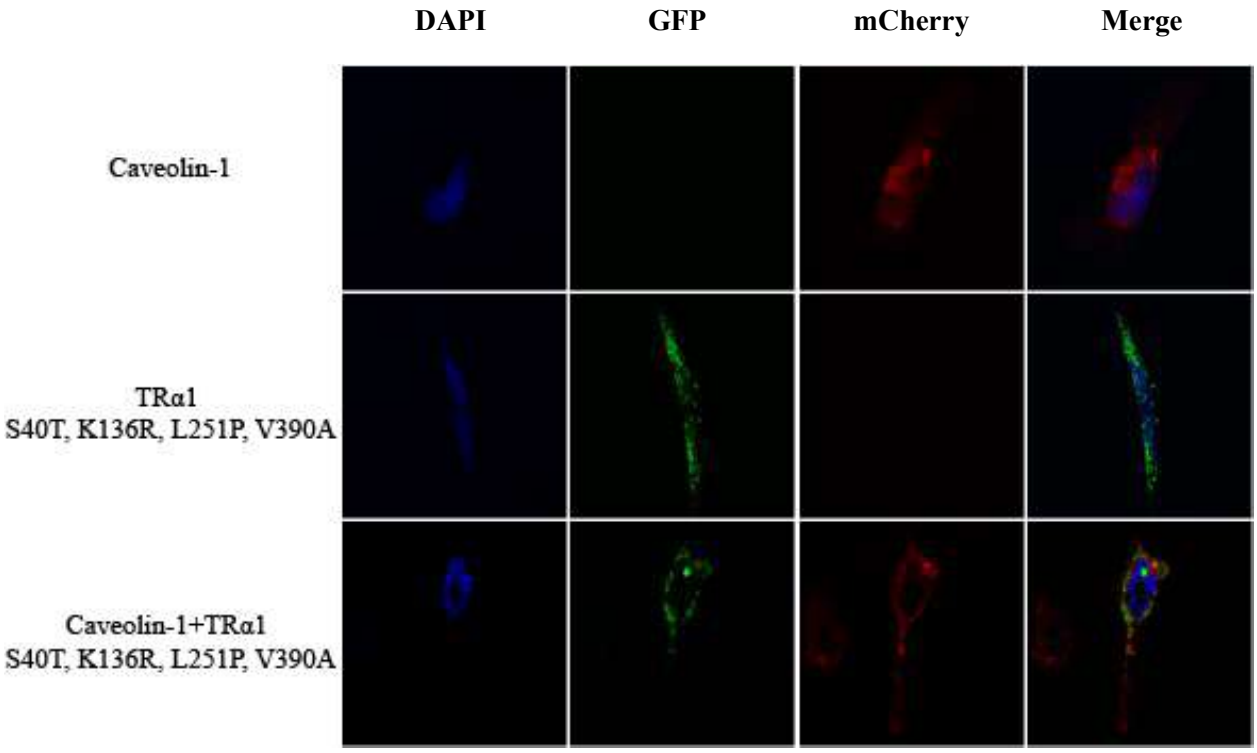
DAPI
GFP
mCherry
Merge
Caveolin-1
TRα1
S40T, K136R, L251P, V390A
Caveolin-1+TRα1
S40T, K136R, L251P, V390A

(B)

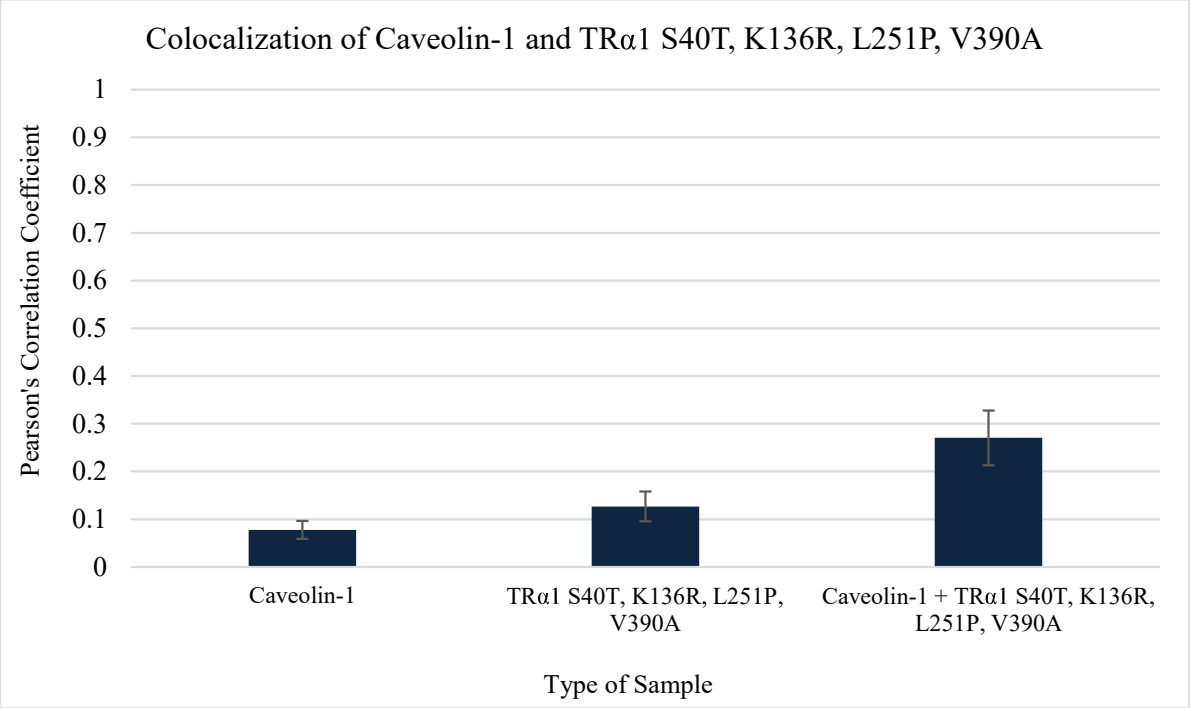

Figure 7: HeLa cells were transfected with mCherry-caveolin-1 and GFP-TRα1 S40T, K136R, L251P, V390A expression plasmids, fixed, and stained with DAPI. (A) In the images, red fluorescence indicates mCherry-caveolin-1, green fluorescence indicates GFP-TRα1, and blue fluorescence indicates DAPI-stained nucleus. (B) In the graph, the bars indicate PCC of caveolin 1, mutant TRα1, and caveolin 1+mutant TRα1. Error bars indicate ± SEM (n=3 biologically independent replicates, at least 25 cells scored per replicate).

.

Discussion

It has previously been shown that mutations in TR may be contributing to the development of particular types of cancer, including hepatocellular carcinoma and papillary thyroid cancer. However, the reasons for this association are unclear. This thesis has demonstrated that certain cancer-associated mutations in the NLSs or NESs of TRα1 can lead to an increased cytoplasmic distribution of the mutant receptor relative to wild-type TRα1, and can aggregate throughout the cell, which could disrupt gene expression.

More specifically, TRα1 S40T, K136R, L251P, V390A; TRα1 L251P; and TRα1 A225G, D246N, E350K showed a higher cytoplasmic distribution and a greater formation of aggregates, compared to WT TRα1. With this finding, it is important to note that even a single point mutation (L251P) in TRα1 can drastically alter the localization of TRα1. Such a difference in localization may occur in this particular mutant because, unlike leucine, proline forms a nitrogen-containing ring and introduces kinks into α-helices. Considering that L251P is a mutation in the NES-H3/NES-H6 region of TRα1 and it has been previously shown that TRα1 S40T, K136R, L251P, V390A has no T_3 binding, the formation of kinks in the LBD may be disrupting the binding of T_3 to TR and interfering with target gene transcription. These kinks could also be contributing to the formation of aggregates.

In terms of TRα1 A225G, D246N, E350K, upon first look, it may seem as if it is unlikely that the change from alanine (a small non-polar amino acid) to glycine (a small non-polar amino acid) is leading to the observed mislocalization. However, there is evidence suggesting that the stability of a helix with alanine versus glycine varies based on the location of the helix within a protein and on their surrounding amino acids. More specifically, glycine leads to a more stable helix when the helix is at an N-terminal or a C-terminal location, but alanine allows for a more

stable helix when the helix is located internally within a protein (Serrano et al., 1992). Since the mutation A225G occurs internal to TRα1, it may be destabilizing TRα1, contributing to mislocalization and formation of aggregates. The change from aspartic acid (a negatively charged amino acid) to asparagine (a polar, neutral amino acid) located in the NES-H3/NES-H6 region of LBD is also likely to be altering the cellular distribution of TR, since the structure and possible interactions of these amino acids are different. The conversion of glutamic acid (a negatively charged amino acid) to lysine (a positively charged amino acid) in the LBD could also be contributing to the formation of aggregates, but it is less likely that it is leading to higher cytoplasmic distribution since the mutation is not in an NLS or NES region. Both D246N and E350K could be leading to the formation of aggregates since their structures and interactions would be different.

The TRα1 mutations L251P, A225G, and D246N all occur in the NES-H3/NES-H6 region of LBD. Considering that the NLSs and NESs are conserved among vertebrate species, the mutations in the NES region may be leading to decreased affinity for exportins. However, reduced affinity for exportins does not explain why the TRα1 mutants are showing a decreased nuclear-to-cytoplasmic ratio compared to WT TRα1; exportins transport TRα1 out of the nucleus, and reduced affinity to exportins would indicate that the nuclear-to-cytoplasmic ratio of TRα1 would be higher than that of WT TRα1. One possibility for this unexpected cellular distribution may be that the mutations in the NES-H3/NES-H6 region interact with the other amino acids in TRα1 and are close enough to the hinge domain that they could be altering the structure of the NLSs of TRα1, disrupting the binding of importins to the NLSs. Such disruption would prevent TRα1 from entering the nucleus, leading to the observed decrease in its nuclear-to-cytoplasmic ratio. Another possibility is that the mutations in the NES region may be leading

to increased affinity for exportins. In this case, the exportins would more efficiently transport TRα1 mutant out of the nucleus, leading to a decrease in nuclear-to-cytoplasmic ratio. However, increased affinity is unlikely because, although NES consensus sequences are not well-defined, it has been repeatedly observed that they tend to be hydrophobic (Kosugi et al., 2008); the TRα1 mutations L251P, A225G, and D246N probably do not increase hydrophobicity of the NES-H3/NES-H6 region because proline and asparagine are not hydrophobic, and alanine and glycine are both hydrophobic.

In addition, TRα1 G24E had a greater cytoplasmic distribution, compared to WT TRα1. Since this mutation is in the NLS-2 region of A/B domain, the NLS-2 of the TR mutant may not be recognized by an importin and the TR mutant may not be transported into the nucleus as efficiently as the WT TRα1. In addition, alanine is a non-polar amino acid while glutamic acid is a negatively charged amino acid, which could alter the structure of the TRα1 mutant and possibly interfere with the binding of T_3 to the TRα1 mutant.

In contrast, the cellular distributions of TRα1 E213D and TRα1 K74E were similar to that of WT TRα1. While E213D is located in the NES-H3/NES-H6 region of LBD, both glutamic acid and aspartic acid are negatively charged amino acids, indicating that the structure of TRα1 may not be affected enough to change the localization. With regards to TRα1 K74E, although there is a conversion from lysine (a positively charged amino acid) to glutamic acid (a negatively charged amino acid), the mutation does not occur in an NLS or NES region so the localization of the TRα1 mutant is not affected.

In summary, it seems as if mutations in the NLS or NES regions of TRα1 that alter tertiary structure are likely to lead to a decrease in the nuclear-to-cytoplasmic distribution of TRα1. If these mutations occur in the LBD, then the mutant TRα1 proteins are likely to form aggregates.

Considering that TRα1 is crucial for the regulation of growth and development, such alterations in the intracellular distribution of TRα1 may disrupt proper gene expression and contribute to cancer progression.

Protein Aggregation Diseases

Protein aggregation diseases are diseases that are known to develop or progress due to aggregation of misfolded proteins within or outside cells. These include neurodegenerative diseases such as Alzheimer's disease, Parkinson's disease, Huntington's disease, and Amyotrophic Lateral Sclerosis (ALS), which are characterized by the aggregation of Aβ-peptide, α-synuclein, Huntingtin, and ubiquitinated proteins, respectively. Protein aggregation occurs when hydrophobic amino acids that are normally buried within the protein become exposed to the aqueous environment inside the cell. When multiple misfolded proteins with exposed hydrophobic amino acids interact with one another, hydrophobic forces cause the proteins to aggregate. Protein aggregation can also occur if misfolded proteins have a greater tendency to form β-sheets or have a lower net charge than wild-type proteins (Kumar et al., 2016). In neurodegenerative diseases, protein aggregates have often been associated with mitochondrial dysfunction, oxidative stress, and chronic inflammation. (Rego and Oliveira, 2003). This association is interesting because chronic inflammation is a major risk factor for many types of cancer, including hepatocellular carcinoma (Coussens and Werb, 2002). In this way, the TRα1 mutant aggregates could be leading to oxidative stress and chronic inflammation, contributing to the progression of certain types of cancers, such as hepatocellular carcinoma.

Future Directions

Based on the data presented in this thesis, mutations in the NES-H3/NES-H6 region of the LBD of TRα1 are likely to lead to mislocalization of TRα1. Considering the fact that the mutations could be leading to changes in structure and function of TRα1, it would be interesting to observe the altered structures of TRα1 by utilizing protein prediction software. Examining the modified structures may allow for a better understanding of the reasons for mislocalization. In the instances in which TRα1 has multiple mutations, using protein prediction software would help clarify the interactions between the regions with mutations. Predicting the protein structure could also reveal the possible causes of aggregate formation. Previous research has shown that aggregate formation is more likely when proteins are highly hydrophobic, tend to form β-sheets, and have low net charge (Kumar et al., 2016). Also, there is evidence suggesting that regions of proteins that have reverse turns are important for proper protein folding. All of these factors could be accounted for when visualizing and analyzing mutated proteins through protein structure prediction.

Furthermore, the aggregates formed by TRα1 mutants should be characterized to further understand the implications of the aggregates. Characterization of small aggregates can be conducted by utilizing mass spectrometry—a technique that ionizes samples and determines their mass-to-charge ratios, allowing unknown compounds in a sample to be identified.

Lastly, it has been previously shown that formation of aggregates may lead to mitochondrial dysfunction and overexpression of proinflammatory cytokines, which can cause chronic inflammation. For example, it has been demonstrated that misfolded protein aggregates can lead to accumulation of metabolites; both the aggregates and metabolites can then localize to mitochondria-associated membranes and trigger ER stress, stimulate production of reactive

oxygen species, and activate NLRP3 inflammasome (Missiroli et al., 2018). Since TRα1 S40T, K136R, L251P, V390A and TRα1 A225G, D246N, E350K were found to form aggregates, it would be interesting to analyze HeLa cells that are cotransfected with a TRα1 mutant and a mitochondrial marker to check for possible colocalization.

References

Adler, Jeremy, and Ingela Parmryd. "Quantifying Colocalization by Correlation: The Pearson Correlation Coefficient is Superior to the Mander's Overlap Coefficient." *Cytometry Part A*, vol. 77, no. 8, 2010, pp. 733-742.

Anyetei-Anum, Cyril S., Vincent R. Roggero, and Lizabeth A. Allison. "Thyroid Hormone Receptor Localization in Target Tissues." *Journal of Endocrinology*, vol. 237, no. 1, 2018, pp. R19-R34.

Aranda, Ana, and Angel Pascual. "Nuclear Hormone Receptors and Gene Expression." *Physiological Reviews*, vol. 81, no. 3, 2001, pp. 1269-1304.

Beck, Martin, and Ed Hurt. "The Nuclear Pore Complex: Understanding its Function through Structural Insight." *Nature Reviews Molecular Cell Biology*, vol. 18, no. 2, 2017, pp. 73.

Bochukova, Elena, et al. "A Mutation in the Thyroid Hormone Receptor Alpha Gene." *New England Journal of Medicine*, vol. 366, no. 3, 2012, pp. 243-249.

Bonamy, Ghislain M., Anne Guiochon-Mantel, and Lizabeth A. Allison. "Cancer Promoted by the Oncoprotein v-ErbA may be due to Subcellular Mislocalization of Nuclear Receptors." *Molecular Endocrinology*, vol. 19, no. 5, 2005, pp. 1213-1230.

Bondzi, Cornelius, et al. "Recruitment of the Oncoprotein v-ErbA to Aggresomes." *Molecular and Cellular Endocrinology*, vol. 332, no. 1-2, 2011, pp. 196-212.

Cook, Atlanta, et al. "Structural Biology of Nucleocytoplasmic Transport." *Annu.Rev.Biochem.*, vol. 76, 2007, pp. 647-671.

Coussens, Lisa M., and Zena Werb. "Inflammation and Cancer." *Nature*, vol. 420, no. 6917, 2002, pp. 860.

Davis, Paul J., Fernando Goglia, and Jack L. Leonard. "Nongenomic Actions of Thyroid Hormone." *Nature Reviews Endocrinology*, vol. 12, no. 2, 2016, pp. 111.

Devos, D., et al. "Simple Fold Composition and Modular Architecture of the Nuclear Pore Complex." *Proceedings of the National Academy of Sciences of the United States of America*, vol. 103, no. 7, 2006, pp. 2172-2177.

Dobson, Christopher M. "Protein Folding and Misfolding." *Nature*, vol. 426, no. 6968, 2003, pp. 884.

Hayer, Arnold, et al. "Biogenesis of Caveolae: Stepwise Assembly of Large Caveolin and Cavin Complexes." *Traffic*, vol. 11, no. 3, 2010, pp. 361-382.

Jucker, Mathias, and Lary C. Walker. "Self-Propagation of Pathogenic Protein Aggregates in Neurodegenerative Diseases." *Nature*, vol. 501, no. 7465, 2013, pp. 45.

Kalyanaraman, H., et al. "Nongenomic Thyroid Hormone Signaling Occurs through a Plasma Membrane-Localized Receptor." *Science Signaling*, vol. 7, no. 326, 2014, pp. ra48.

Kosugi, Shunichi, et al. "Nuclear Export Signal Consensus Sequences Defined using a localization-based Yeast Selection System." *Traffic*, vol. 9, no. 12, 2008, pp. 2053-2062.

Kumar, Vijay, et al. "Protein Aggregation and Neurodegenerative Diseases: From Theory to Therapy." *European Journal of Medicinal Chemistry*, vol. 124, 2016, pp. 1105-1120.

Lazar, M. A. "Thyroid Hormone Action: A Binding Contract." *The Journal of Clinical Investigation*, vol. 112, no. 4, 2003, pp. 497-499.

Lin, Kwang-Huei, et al. "Expression of Mutant Thyroid Hormone Nuclear Receptors in Human Hepatocellular Carcinoma Cells." *Molecular Carcinogenesis*, vol. 26, no. 1, 1999, pp. 53-61.

Mavinakere, M. S., et al. "Multiple Novel Signals Mediate Thyroid Hormone Receptor Nuclear Import and Export." *The Journal of Biological Chemistry*, vol. 287, no. 37, 2012, pp. 31280-31297.

Missiroli, Sonia, et al. "Mitochondria-Associated Membranes (MAMs) and Inflammation." *Cell Death & Disease*, vol. 9, no. 3, 2018, pp. 329.

Nascimento, Alessandro S., et al. "Structural Rearrangements in the Thyroid Hormone Receptor Hinge Domain and their Putative Role in the Receptor Function." *Journal of Molecular Biology*, vol. 360, no. 3, 2006, pp. 586-598.

Ortiga-Carvalho, Tania M., et al. "Hypothalamus-pituitary-thyroid Axis." *Comprehensive Physiology*, vol. 6, no. 3, 2011, pp. 1387-1428.

Ortiga-Carvalho, T. M., et al. "Negative Regulation by Thyroid Hormone Receptor Requires an Intact Coactivator-Binding Surface." *The Journal of Clinical Investigation*, vol. 115, no. 9, 2005, pp. 2517-2523.

Puzianowska-Kuznicka, Monika, et al. "Functionally Impaired TR Mutants are Present in Thyroid Papillary Cancer." *The Journal of Clinical Endocrinology & Metabolism*, vol. 87, no. 3, 2002, pp. 1120-1128.

Rego, A. C., and Catarina R. Oliveira. "Mitochondrial Dysfunction and Reactive Oxygen Species in Excitotoxicity and Apoptosis: Implications for the Pathogenesis of Neurodegenerative Diseases." *Neurochemical Research*, vol. 28, no. 10, 2003, pp. 1563-1574.

Serrano, Luis, et al. "Effect of Alanine Versus Glycine in α-Helices on Protein Stability." *Nature*, vol. 356, no. 6368, 1992, pp. 453.

Tang, Yu, et al. "Caveolin-1 is Related to Invasion, Survival, and Poor Prognosis in Hepatocellular Cancer." *Medical Oncology*, vol. 29, no. 2, 2012, pp. 977-984.

Tsai, Ming-Jer, and Bert W. O'Malley. "Molecular Mechanisms of Action of steroid/thyroid Receptor Superfamily Members." *Annual Review of Biochemistry*, vol. 63, no. 1, 1994, pp. 451-486.

Veldman, Matthew B., and X. W. Yang. "Huntington's Disease: Nuclear Gatekeepers Under Attack." *Neuron*, vol. 94, no. 1, 2017, pp. 1-4.

Zhang, Jinsong, and Mitchell A. Lazar. "The Mechanism of Action of Thyroid Hormones." *Annual Review of Physiology*, vol. 62, 2000.

Tang, Y., Zeng, X., He, F., Liao, Y., Qian, N., & Toi, M. (2012). Caveolin-1 is related to invasion, survival, and poor prognosis in hepatocellular cancer. *Medical Oncology, 29*(2), 977-984.

Tsai, M., & O'Malley, B. W. (1994). Molecular mechanisms of action of steroid/thyroid receptor superfamily members. *Annual Review of Biochemistry, 63*(1), 451-486.

Veldman, M. B., & Yang, X. W. (2017). Huntington's disease: Nuclear gatekeepers under attack. *Neuron, 94*(1), 1-4.

Zhang, J., & Lazar, M. A. (2000). The mechanism of action of thyroid hormones. *Annual Review of Physiology, 62*